# High-Resolution Laser Spectroscopy of CaS: Deperturbation Analysis of the $A^1\Sigma^+-X^1\Sigma^+$ Transition†

**Todd C. Melville and John A. Coxon***

*Department of Chemistry, Dalhousie University, Halifax, NS Canada B3H 4J3*

*Received: November 20, 2001; In Final Form: March 12, 2002*

The $A^1\Sigma^+-X^1\Sigma^+$ electronic transition in CaS has been rotationally analyzed using high-resolution, laser excitation spectroscopy. Doppler-limited spectra were recorded for the 0−0, 1−0, 1−1, 2−1, 3−1, 3−2, 4−2, 4−3, 5−3, 5−4, 6−4 and 6−5 bands with a measurement precision of approximately 0.003 $cm^{-1}$. In total, more than 1200 line positions have been measured, assigned and employed in least-squares fits of molecular parameters. The $A^1\Sigma^+$ state is extensively perturbed and level crossings have been identified and analyzed in the $A^1\Sigma^+$ $v = 3$, 4, 5, and 6 vibrational levels. The perturbations are believed to arise from interactions of the $A^1\Sigma^+$ state with the $a^3\Pi$ and $A'^1\Pi$ states. Term values and effective rotational parameters for the perturbing states are obtained through a partial deperturbation analysis of the perturbed bands. Estimated values of the principal molecular parameters are $T_{00} = 15194.428(2)$ $cm^{-1}$, $R_e' = 2.38626(16)$ Å, and $\omega_e' = 409.077(9)$ $cm^{-1}$ for the $A^1\Sigma^+$ state, and $R_e'' = 2.31770(14)$ Å and $\omega_e'' = 462.273(12)$ $cm^{-1}$ for the $X^1\Sigma^+$ state.

## Introduction

The alkaline-earth monosulfides CaS, SrS, and BaS have been the subject of a number of spectroscopic investigations.[1−11] However, their electronic structures, and more specifically, their low-lying electronic states, are not as well characterized as those of the alkaline-earth monoxides.[12−18] With the exception of CaS,[1] all of the known low-lying excited states of the alkaline earth monoxides and monosulfides are extensively perturbed. Our interest in perturbations observed recently in YbS[19−21] spurred the present reinvestigation of the $A^1\Sigma^+-X^1\Sigma^+$ electronic transition in CaS.

Blues and Barrow were the first to record the absorption spectrum of the $A^1\Sigma^+-X^1\Sigma^+$ electronic transition of CaS in the red region of the spectrum.[1] These authors rotationally analyzed the 0−0, 1−0, 1−1, 0−1, 1−2 and 2−1 bands at high resolution to $J \approx 200$. They obtained equilibrium values for the vibrational and rotational parameters of the $A^1\Sigma^+$ and $X^1\Sigma^+$ states, but did not observe any perturbations.[1] Very recently, Andersson and Davis extended this work by recording the emission spectrum of CaS from a tube furnace (employing the labeling $B^1\Sigma^+-X^1\Sigma^+$ for the same transition).[5] Though they recorded a large number of rotational lines from bands that sampled $v = 0-5$ in both electronic states, they did not report any perturbations in the observed spectra. Other work on CaS includes a high-resolution laser study by Jarman, Hailey and Bernath[2] of three electronic transitions in the blue region of the spectrum; these transitions were assigned as $G^1\Pi-X^1\Sigma^+$, $F^1\Pi-X^1\Sigma^+$, and $f^3\Pi-X^1\Sigma^+$. In addition, there has been a millimeter wave study of the ground electronic state by Takano, Yamamoto and Saito[3] and a study of CaS in a solid argon matrix by Martin and Schaber.[4] The previous high-resolution studies were very helpful in the present work because they provided accurate constants for the $X^1\Sigma^+$ state up to $v = 7$, allowing us to use ground-state combination differences in assigning the $A^1\Sigma^+$ state perturbations.

In addition to the aforementioned experimental work, Partridge, Langhoff and Bauschlicher have performed ab initio calculations on the alkaline-earth monosulfides to determine the spectroscopic constants $T_e$, $R_e$, $\omega_e$ and $D_e$ for the $X^1\Sigma^+$, $a^3\Pi$ and $A'^1\Pi$ states.[6] The calculations predicted $T \approx 7000$ $cm^{-1}$ for the $a^3\Pi$ and $A'^1\Pi$ states, significantly below the energy of the $A^1\Sigma^+$ state, which has $T \approx 15\,000$ $cm^{-1}$. The predicted position of the $A'^1\Pi$ state is in good agreement with a tentative observation of this state at low-resolution by Jarman, Hailey and Bernath,[2] though there has been no conclusive identification or analysis of the $a^3\Pi$ and $A'^1\Pi$ states.

The present work is the first high-resolution laser study of the $A^1\Sigma^+-X^1\Sigma^+$ electronic transition in CaS. The analysis of the A−X system has resulted in the identification of a number of level crossings in the $A^1\Sigma^+$ state, and effective parameters for the perturbing states are determined from a partial deperturbation analysis.

## Experimental Method

Gas-phase CaS was produced in a Broida-type oven[22] by the reaction of OCS with Ca metal vapor, entrained in a flow of argon carrier gas. Total pressures in the oven ranged from 3 to 5 Torr, with the oxidant gas making up <1% of this pressure. Carbon disulfide, $CS_2$, was also tested as a possible oxidant, but the resulting signal was not as strong as that obtained for OCS. The $A^1\Sigma^+-X^1\Sigma^+$ bands were probed with the output of a Coherent 699-29 ring dye laser operating in single-frequency mode with DCM laser dye. Laser induced fluorescence (LIF) was observed perpendicular to the exciting laser beam and imaged onto the entrance slit of a 1.26 m Spex monochromator. The laser beam was modulated at 540 Hz with a mechanical chopper to allow phase-sensitive detection of the LIF and suppress unwanted chemiluminescence. The spectrometer is

† Part of the special issue "Donald Setser Festschrift".

* Corresponding author: E-mail: jacoxon@is.dal.ca. Tel: (902) 494-3716. Fax: (902) 494-1310.

10.1021/jp014299z CCC: $22.00 
Published on Web 04/26/2002

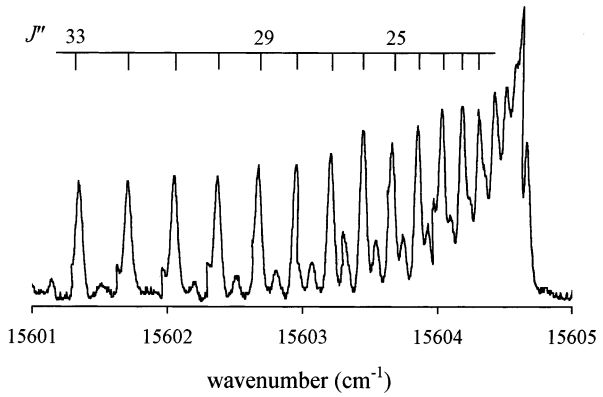


**Figure 1.** Portion of the 1−0 band of the CaS $A^1\Sigma^+-X^1\Sigma^+$ transition near the *R*-branch head.

equipped with an RCA GaAs C31034-02 photomultiplier, cooled to −20 °C. During experiments in which the laser was scanned, the spectrometer served as a narrow band-pass filter for the photoelectric detection of LIF. An $I_2$ fluorescence spectrum was recorded simultaneously and compared to the standard $I_2$ atlas for calibration;[23] the line positions in the atlas were corrected by −0.0056 $cm^{-1}$, as proposed by Gerstenkorn and Luc.[24] The experiments were Doppler-limited and spectral line widths were on the order of 0.03 $cm^{-1}$. The precision of measurements in similar previous work with this arrangement is typically about 0.003 $cm^{-1}$.

## Results and Deperturbation Analysis

The $A^1\Sigma^+-X^1\Sigma^+$ 0−0, 1−0, 1−1, 2−1, 3−1, 3−2, 4−2, 4−3, 5−3, 5−4, 6−4, and 6−5 bands observed in the present work consist of red-degraded P- and R-branches. Typically, we were able to record rotational lines for both branches up to $J \approx 90$, with the R-branch forming a head at relatively low $J$ (≈15). Figure 1 shows a portion of the 1−0 band R-branch in the region of the band head. Once the spectra were recorded and measured, assignment of the rotational numbering, $J$, was achieved using the standard combination differences. In addition, it was possible to observe the "first lines" of several bands. The data for individual bands were then employed in a least-squares fitting program that contains the usual analytical expression for the term values of $^1\Sigma^+$ states. For each band, the fitted parameters were the band origin $\upsilon_0$, and the rotational parameters $B_\upsilon$ and $D_\upsilon$ for both the upper and lower states.

While the initial fits of the 0−0, 1−0, 1−1 and 2−1 bands had standard deviations on the order of 0.003 $cm^{-1}$, the remainder of the bands possessed anomalously large standard deviations, with many lines exhibiting systematically large residuals. It was immediately obvious that the $A^1\Sigma^+$ state $\upsilon$ = 3, 4, 5 and 6 levels are extensively perturbed. Careful inspection revealed no perturbations in the $\upsilon = 0$, 1 and 2 vibrational levels up to $J \approx 90$, confirming Blues and Barrow's work on this system.[1] Figure 2 shows a portion of the 6−4 band in the region of a perturbation in the P-branch. A plot of the residuals of the line positions before deperturbation of the 6−4 band is given in Figure 3. To determine accurate positions of the crossing points, and to obtain more information about the nature of the perturbers, we modified the band-fitting program to incorporate perturbing states described by their term values ($T_P$) and rotational parameters, $B_P$ and $D_P$. Interaction between the $A^1\Sigma^+$ state and a perturber ($P_i$) could be modeled either as a homogeneous ($\Delta\Omega = 0$, $J$-independent) perturbation or a heterogeneous ($\Delta\Omega = \pm 1$, $J$-dependent) perturbation. To properly represent the crossings of the $A^1\Sigma^+$ and perturbing

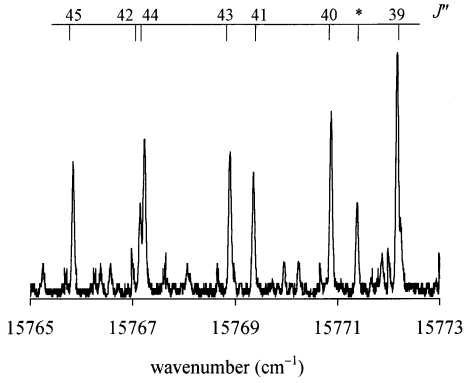


**Figure 2.** Portion of the P-branch of the CaS $A^1\Sigma^+-X^1\Sigma^+$ 6−4 band. The spectrum is shown near the $A^1\Sigma^+ \sim P_7$ level crossing. The line labeled with an asterisk is an "extra line" assigned as P(42).

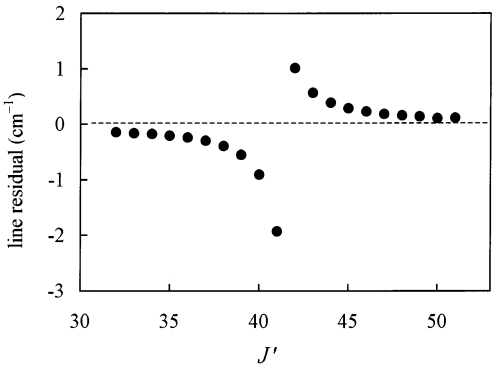


**Figure 3.** Plot of the residuals of the line positions near the $A^1\Sigma^+ \sim P_7$ crossing point in the 6−4 band of CaS. The residuals represent the differences between the observed line positions and those calculated before deperturbation.

states, very careful selection of the trial parameters was essential, and it was necessary to keep the centrifugal distortion constants for the perturbing states, $D_P$, fixed during the deperturbation fits. Because we had no additional knowledge of the perturbing states, we performed separate fits of all the perturbed bands assuming either a heterogeneous or homogeneous interaction. In all cases, both models worked equally well, as discussed further below.

**$A^1\Sigma^+$ State $\upsilon = 3$ Level.** Analysis of the 3−1 and 3−2 bands revealed two level crossings in the $\upsilon' = 3$ level, at $J' = 67.2$ and 77.3. The band-fitting program was modified to fit both crossings simultaneously by solving for each $J$-value a 3 × 3 matrix that describes the interactions between the $A^1\Sigma^+$ state and the perturbing states (referred to hereafter as $P_1$ and $P_2$ for the $J = 67.2$ and 77.3 crossings, respectively). The diagonal components of each matrix contain the standard expressions for Hund's case (a) rotational energy, while the interactions between the $A^1\Sigma^+$ and perturbing states are described in the off-diagonal matrix elements by either α (homogeneous interaction) or $\beta[J(J+1)]^{1/2}$ (heterogeneous interaction). The matrix elements are summarized in Table 1(A). The fitted parameters for the 3−1 and 3−2 bands were the band origins ($\upsilon_0$), the parameters $B_\upsilon$ and $D_\upsilon$ for the $X^1\Sigma$ and $A^1\Sigma$ states, the perturber term values ($T_{P_1}$ and $T_{P_2}$) and rotational constants ($B_{P_1}$ and $B_{P_2}$), and either α or $\beta$ for each crossing. No extra lines associated with either perturbation were identified in these bands; this is discussed further below.

**$A^1\Sigma^+$ State $\upsilon = 4$ Level.** Similar to the $\upsilon' = 3$ level, two perturbations were identified in $\upsilon' = 4$ in the 4−2 and 4−3 bands, with crossing points at $J' = 37.3$ and 50.6 (referred to later as $P_3$ and $P_4$, respectively). The program used to fit the

**TABLE 1: Hamiltonian Matrix Elements**[a]

| 1.(A) | $^1\Sigma$ | $P_1$ | $P_2$ |
|---|---|---|---|
| $^1\Sigma$ | $E_A$ | $\alpha_{P1}$ | $\alpha_{P2}$ |
| $P_1$ | $\alpha_{P1}$ | $E_{P1}$ | 0 |
| $P_2$ | $\alpha_{P2}$ | 0 | $E_{P2}$ |

| 1.(B) | $^1\Sigma$ | $P_1$ |
|---|---|---|
| $^1\Sigma$ | $E_A$ | $\alpha_{P1}$ |
| $P_1$ | $\alpha_{P1}$ | $E_{P1}$ |

| 1.(C) | $^1\Sigma$ | $P_1$ | $P_2$ | $P_3$ |
|---|---|---|---|---|
| $^1\Sigma$ | $E_A$ | $\alpha_{P1}$ | $\alpha_{P2}$ | $\alpha_{P3}$ |
| $P_1$ | $\alpha_{P1}$ | $E_{P1}$ | 0 | 0 |
| $P_2$ | $\alpha_{P2}$ | 0 | $E_{P2}$ | 0 |
| $P_3$ | $\alpha_{P3}$ | 0 | 0 | $E_{P3}$ |

[a] $E_A = \upsilon_0 + B_\upsilon J(J+1) - D_\upsilon[J(J+1)]^2$. $E_{P_i} = \upsilon_P + B_P J(J+1) - D_P[J(J+1)]^2$. $\upsilon_0$ is the band origin of the A − X band; $\upsilon_P$ is the band origin of the perturber; $B_\upsilon$, $B_P$ are the rotational constants for the A and perturbing states; $D_\upsilon$, $D_P$ are the centrifugal distortion constants and $\alpha_{P_i}$ is the $A^1\Sigma^+ \sim P_i$ interaction parameter.

perturbations was the same as that for the 3−1 and 3−2 bands, and analogous sets of parameters were determined in the band fits. As for the perturbations in $\upsilon' = 3$, we were unable to identify any extra lines in the spectra.

**$A^1\Sigma^+$ State $\upsilon = 5$ Level.** Analysis of the 5−3 and 5−4 bands revealed the presence of one perturbation in $\upsilon' = 5$ with a crossing point at $J' = 69.6$ ($P_6$). In addition to this, the output of the least-squares fits displayed systematic residuals at low $J$, suggesting a second crossing occurs at $J < 0$ ($P_5$). However, because we observed only one "side" of this level crossing, it was not possible to estimate parameters for $P_5$ in the deperturbation analysis. To obtain the best "deperturbed" estimates for the fitted parameters, the low-$J$ lines involved in the $A^1\Sigma^+ \sim P_5$ interaction were excluded from the fit. The fitting program for the 5−3 and 5−4 bands treated a single level crossing by solving a $2 \times 2$ matrix that describes the interaction between the $A^1\Sigma^+$ and $P_6$ states. The elements for this matrix are given in Table 1(B). No extra lines were observed in either band.

**$A^1\Sigma^+$ State $\upsilon = 6$ Level.** The $\upsilon' = 6$ level is the most extensively perturbed $A^1\Sigma^+$ vibrational level observed in the present work. Level crossings at $J' = 41.1$, 73.4 and 77.4 have been identified unequivocally, and are labeled $P_7$, $P_8$, and $P_9$, respectively. In addition, residual systematic deviations at high $J$ present after deperturbation suggests the possibility of a fourth crossing at $J > 86$. For the $A^1\Sigma^+ \sim P_7$ interaction ($J' = 41.1$ crossing), several extra lines were identified in the 6−4 (5 lines) and 6−5 (2 lines) bands. Following the method of Gerö,[25] the perturbations in $\upsilon' = 6$ are illustrated in Figure 4 by plotting $T/4J$ vs $J$, where $T/4J$ is defined as

$$T/4J = [R(J-2) - R(J-1) + P(J) - P(J+1)]/4J \approx B'' - B' + 6D'' - 2J^2(D'' - D') \quad (1)$$

In unperturbed regions, the $T/4J$ vs $J$ plot is approximately horizontal, with changes occurring in regions of perturbations. The least-squares program for the 6−4 and 6−5 bands involved fitting all three crossings simultaneously, with the extra lines included in the fit. Matrix elements for each $4 \times 4$ matrix employed in the fits are given in Table 1(C).

As can be seen in Table 1, it was assumed that the various perturbers did not interact with each other. To properly fit interactions between the perturbing states, which could be significant, data that directly sample the perturbing states would be required.

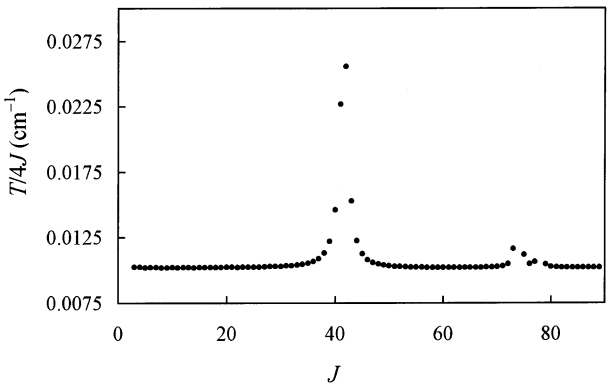


**Figure 4.** Gerö plot[25] of $T/4J$ against $J$ for the 6−4 band of CaS A−X. The plot shows the perturbations in the $\upsilon = 6$ level of the $A^1\Sigma^+$ state (see text for the definition of $T/4J$). Perturbations appear as deviations from the horizontal.

**TABLE 2: Molecular Parameters ($cm^{-1}$) for the $A^1\Sigma^+$ and $X^1\Sigma^+$ States of CaS**[a]

| | $\upsilon$ | $T_\upsilon$ | $B_\upsilon$ | $10^7 D_\upsilon$ |
|---|---|---|---|---|
| $X^1\Sigma^+$ | 0 | 0.0000 | 0.1762501(65) | 1.025(9) |
| | 1 | 458.6662(26) | 0.1754171(62) | 1.027(8) |
| | 2 | 913.7663(34) | 0.1745834(62) | 1.037(8) |
| | 3 | 1365.2921(40) | 0.1737439(62) | 1.048(8) |
| | 4 | 1813.2205(72) | 0.1729083(77) | 1.073(12) |
| | 5 | 2257.5644(79) | 0.1720552(91) | 1.068(22) |
| $A^1\Sigma^+$ | 0 | 15194.4281(18) | 0.1663642(70) | 1.087(14) |
| | 1 | 15601.8649(15) | 0.1657578(65) | 1.092(9) |
| | 2 | 16007.6308(35) | 0.1651530(65) | 1.086(8) |
| | 3 | 16411.7803(30) | 0.1645420(62) | 1.075(8) |
| | 4 | 16814.2570(38) | 0.1639436(60) | 1.080(8) |
| | 5 | 17215.1327(53) | 0.1633341(65) | 1.076(8) |
| | 6 | 17614.3040(74) | 0.1627397(79) | 1.098(13) |

[a] Values in parentheses are standard errors for the corresponding parameters.

In all of the individual deperturbation band fits, the standard deviations of the fits were on the order of 0.003 $cm^{-1}$, indicating that the deviations between the calculated and measured line positions were consistent, on average, with the estimated measurement precision of 0.003 $cm^{-1}$. After fitting the twelve bands individually, the output parameters were then "merged" together in a fashion that is equivalent to a global fit of the entire data set. The merging procedure, which has been described elsewhere,[26,27] takes advantage of redundancies in the fitted parameters. Parameters for the $A^1\Sigma^+$ and $X^1\Sigma^+$ states obtained from the merge fit are given in Table 2, and take account of the $\hat{o}_M \approx 2.4$ of the merge. Constants for the perturbing states, together with the fitted interaction parameters, are given in Table 3. Additional digits beyond those required by the associated standard deviations are given as subscripts to permit calculation of line positions to within the residuals of the fit. As mentioned above, both models (homogeneous and heterogeneous) worked equally well in the deperturbation fits, and in all cases $\alpha_i \approx [J_0(J_0+1)]^{1/2}\beta_i$, where $\alpha_i$ and $\beta_i$ are the homogeneous and heterogeneous interaction parameters, respectively, and $J_0$ is the noninteger crossing point of $P_i$. For simplicity, only the $\alpha_i$'s are reported in Table 3.

The rotational parameters, $B_\upsilon$, for the $A^1\Sigma^+$ and $X^1\Sigma^+$ states follow regular trends with increasing vibrational quantum number, and it was possible in the merge fit to estimate equilibrium values of the constants from the twelve bands; these are given in Table 4.

**TABLE 3: Parameters ($cm^{-1}$) for the $A^1\Sigma^+ \sim P_i$ Interactions in CaS[a]**

| $A^1\Sigma^+(v)$ | $P_i$ | $T_{P_i}$ | $B_{P_i}$ | $10^7 D_{P_i}$ | $\alpha_{P_i}$ | $J_0$ | label |
|---|---|---|---|---|---|---|---|
| 3 | $P_1$ | $16546._{40}(34)$ | $0.1351_{72}(74)$ | [1.0] | 0.296(36) | 67.2 | I($v$) |
| 3 | $P_2$ | $16627._{26}(46)$ | $0.1288_4(74)$ | [1.0] | 0.229(36) | 77.3 | II($v'$) |
| 4 | $P_3$ | $16850._{680}(6)$ | $0.1383_{88}(38)$ | [1.0] | 0.520(34) | 37.3 | I($v$+1) |
| 4 | $P_4$ | $16890._{20}(6)$ | $0.1348_{79}(22)$ | [1.0] | 0.483(18) | 50.6 | II($v'$+1) |
| 5 | $P_5$ | | | | | <0 | |
| 5 | $P_6$ | 17373.23(6) | 0.131152(13) | [1.0] | 1.064(5) | 69.6 | III($v$) |
| 6 | $P_7$ | $17691.45_8(11)$ | 0.118133(67) | [1.0] | 2.1051(22) | 41.1 | |
| 6 | $P_8$ | $17950._{22}(50)$ | $0.1012_1(94)$ | [1.0] | $1.12_5(8)$ | 73.4 | |
| 6 | $P_9$ | $17719._{40}(65)$ | $0.145_{37}(11)$ | [1.0] | $0.30_5(8)$ | 77.4 | |

[a] Values in parentheses are standard errors for the corresponding parameter in units of the least significant digit shown in regular type. Additional digits are given as subscripts to permit calculation of line positions to within the residuals of the fit. Values in square brackets were held fixed in the fits.

**TABLE 4: Molecular Parameters ($cm^{-1}$) for the $A^1\Sigma^+$ and $X^1\Sigma^+$ States of CaS[a]**

| | $X^1\Sigma^+$ | $A^1\Sigma^+$ |
|---|---|---|
| $T_{00}$ | 0.0 | 15194.4281(18) |
| $B_e$ | 0.176683(21) | 0.166676(22) |
| $10^4\alpha_e$ | 8.393(34) | 6.070(28) |
| $\omega_e$ | 462.273(12) | 409.077(9) |
| $\omega_e x_e$ | 1.7926(17) | 0.8231(12) |
| $R_e$ (Å) | 2.31770(14) | 2.38626(16) |

[a] Values in parentheses are standard errors for the corresponding parameters.

## Discussion

As mentioned above, all of the perturbations (except $P_5$) were fit assuming either a homogeneous or heterogeneous model, and in all cases the fits were equally satisfactory. It is apparent that with the current measurement precision, the two models are found equally effective on account of the relatively high $J$-values of the perturbations and the rather small ranges of $J$ for which significant perturbations are observed. It should be noted that a similar situation exists for the perturbations in SrS[7] and YbS.[19]

It is somewhat disappointing that we were unable to identify extra lines associated with most of the perturbations, as this would provide crucial data and information about the perturbing states. The presence of overlapping bands in most of the spectra usually precluded the assignment of extra lines, as there was often blending of the rotational lines between different bands. In addition, spectra associated with the perturbations that occur at high-$J$ have a rather poor signal/noise ratio.

In the absence of any additional information about the perturbing states, beyond that deduced herein from the deperturbation analyses, further discussion remains equivocal. On the basis of the known electronic structure of the alkaline-earth monoxides,[12−18] the perturbations in the $A^1\Sigma^+$ state of CaS can be attributed to the low-lying $a^3\Pi$ and $A'^1\Pi$ states. These states have been identified tentatively for CaS at low-resolution by Jarman et al.,[2] though no rotational analysis has been carried out. Because of mixing between the basis functions of the $^3\Pi$ state (nominally $^3\Pi_0$, $^3\Pi_1$ and $^3\Pi_2$), all three substates can interact with the $A^1\Sigma^+$ state.[12] Accordingly, four states, $A'^1\Pi$, $a^3\Pi_0$, $a^3\Pi_1$ and $a^3\Pi_2$, can perturb the $A^1\Sigma^+$ state, with the $A^1\Sigma^+ \sim a^3\Pi_2$ interaction likely being the weakest.

In the present work we have identified unequivocally nine perturbations in the $A^1\Sigma^+$ state $v = 3-6$ vibrational levels. As a first step in understanding the identity of the perturbing states, the vibration−rotational energies of the $A^1\Sigma^+$ and perturbing states are plotted as a function of $J(J+1)$ in Figure 5. It seems reasonable, based on Figure 5, to assume that the pairs of perturbers that cross the $A^1\Sigma^+$ $v = 3$ and 4 levels ($P_1/P_2$ and $P_3/P_4$) come from two distinct states. In other words, $P_1$ and $P_3$ are successive vibrational levels from the same perturbing state (I), and $P_2$ and $P_4$ are successive vibrational levels from a second perturbing state (II). It would be expected that the perturbing states have approximately the same vibrational spacing, and it is found that $\omega^{I} \approx \omega^{II} \approx 330$ $cm^{-1}$ (with an estimated uncertainty on the order of 10 $cm^{-1}$). Values for the vibrational spacings were obtained from the separation of the vibrational levels near the perturbations, thereby reducing the error associated with extrapolation to $J = 0$. It should be noted that the relative strengths of the perturbations are consistent with the above assignments. If the two states (I and II) arise from the low-lying $a^3\Pi$ and $A'^1\Pi$ states with $T_e' \approx 7000$ $cm^{-1}$, then the quantum number of the perturbing vibrational levels would be quite high (≈25−30). This situation is plausible despite the fact that no perturbations were observed in $A^1\Sigma^+$ $v = 0-2$, since crossings in these vibrational levels may have energy shifts that are too small to observe with the current measurement accuracy, or that of the previous work on this system by Blues and Barrow.[1]

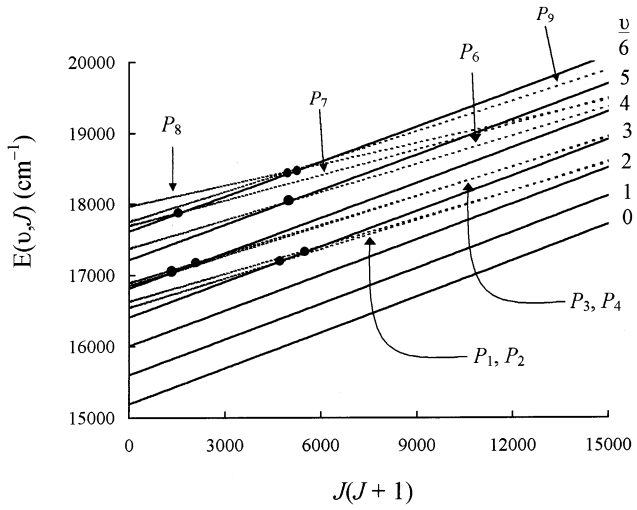


**Figure 5.** Dependence of vibration−rotation energy on $J(J+1)$ for the $A^1\Sigma^+$ state of CaS (solid lines) and the perturbers $P_1-P_9$ (dashed lines). Note: $P_5$ occurs at $J < 0$ and is therefore not shown. Observed level crossings are indicated by ●.

Unfortunately, an understanding of the perturbations in $v = 5$ and 6 is not as obvious as $P_1-P_4$. By extrapolation of the perturbing states I and II by the estimated vibrational frequency $\omega_P \approx 330$ $cm^{-1}$, it is found that the vibrational levels above those responsible for $P_3/P_4$ would cross in the energy region below the $J = 0$ level in $A^1\Sigma^+$ $v = 5$. These level(s) could be responsible for $P_5$, which "crosses" $v = 5$ at $J < 0$, though this interpretation should be regarded as tentative.

Based on its vibration−rotational energy, $P_6$ does not appear to arise from either perturbing state identified above (I or II), and therefore, it is assumed to come from a third state (III). From the rotationless energy separation of $P_6$ and $P_7$ (≈320 $cm^{-1}$), it is tempting to presume that both of these perturbations arise from the same electronic state (III). However, the rotational constants for the two perturbing levels are significantly different (see Table 3) and we hesitate to draw any firm conclusions about the identity of these perturbers.

With relatively little data sampling the $P_8$ and $P_9$ perturbations, and their close proximity to one another, least-squares fits of the bands involving these level crossings was difficult. In fact, the lack of data likely contributes to the inconsistency in the fitted rotational parameters for these two perturbing levels (Table 3). One must also consider that the model employed,

which assumes no interactions between the perturbers, may be inadequate for properly fitting perturbations so close to one another.

In summary, we have employed high-resolution laser spectroscopic techniques to investigate the $A^1\Sigma^+-X^1\Sigma^+$ transition in CaS. Nine perturbations have been observed in the $v = 3-6$ levels of the $A^1\Sigma^+$ state, and through a partial deperturbation analysis of the perturbed bands, we have obtained molecular parameters for the perturbing levels. Further work that directly samples the low-lying $a^3\Pi$ and $A'^1\Pi$ states in CaS is required to better understand the manifold of electronic states in this molecule and to unequivocally assign the perturbations observed in the present work.

**Acknowledgment.** T.C.M. thanks the Walter C. Sumner Foundation for a graduate scholarship at Dalhousie University. Support for this work via research and equipment grants from the Natural Sciences and Engineering Research Council of Canada is gratefully acknowledged.

**Supporting Information Available:** A complete list of all line positions used in the fits (≈1200), as well as residuals between the measured lines and line positions calculated using the parameters in Tables 2 and 3, is available free of charge via the Internet at http://pubs.acs.org.

## References and Notes

(1) Blues, R. C.; Barrow, R. F. *Trans. Faraday Soc.* **1969**, *65*, 646.
(2) Jarman, C. N.; Hailey, R. A.; Bernath, P. F. *J. Chem. Phys.* **1992**, *96*, 5571.
(3) Takano, S.; Yamamoto, S.; Saito, S. *Chem. Phys. Lett.* **1989**, *159*, 563.
(4) Martin, T. P.; Schaber, H. *Spectrochim. Acta A* **1982**, *38*, 655.
(5) Andersson, N.; Davis, S. P. *Phys. Scripta* **2001**, *64*, 446.
(6) Partridge, H.; Langhoff, S. R.; Bauschlicher, C. W. *J. Chem. Phys.* **1988**, *88*, 6431.
(7) Pinalto, F. S.; Brazier, C. R.; O'Brien, L. C.; Bernath, P. F. *J. Mol. Spectrosc.* **1988**, *132*, 80.
(8) Marcano, M.; Barrow, R. F. *Trans. Faraday Soc.* **1970**, *66*, 1917.
(9) Cummins, P. G.; Field, R. W.; Renhorn, I. *J. Mol. Spectrosc.* **1981**, *90*, 327.
(10) Barrow, R. F.; Burton, W. G.; Jones, P. A. *Trans. Faraday Soc.* **1971**, *67*, 902.
(11) Morbi, Z.; Bernath, P. F. *J. Mol. Spectrosc.* **1995**, *171*, 210.
(12) Field, R. W. *J. Chem. Phys.* **1974**, *60*, 2400.
(13) Gottscho, R. A.; Koffend, J. B.; Field, R. W. *J. Mol. Spectrosc.* **1980**, *82*, 310.
(14) Fosca, C.; Poclet, A.; Pinchemel, B.; Le Roy, R. J.; Bernath, P. F. *J. Mol. Spectrosc.* **2000**, *203*, 330.
(15) Li, H.; Skelton, R.; Fosca, C.; Pinchemel, B.; Bernath, P. F. *J. Mol. Spectrosc.* **2000**, *203*, 188.
(16) Lagerqvist, A.; Lind, E.; Barrow, R. F. *Proc. Phys. Soc. A* **1950**, *63*, 1132.
(17) Hultin, M.; Lagerqvist, A. *Ark. Fys.* **1950**, *2*, 471.
(18) Li, H.; Focsa, C.; Pinchemel, B.; Le Roy, R. J.; Bernath, P. F. *J. Chem. Phys.* **2000**, *113*, 3026.
(19) Melville, T. C.; Coxon, J. A.; Linton, C. *J. Chem. Phys.* **2000**, *113*, 1771.
(20) Melville, T. C.; Coxon, J. A. *Chem. Phys. Lett.* **2000**, *318*, 454.
(21) Melville, T. C.; Linton, J. A.; Coxon, J. A. *J. Mol. Spectrosc.* **2000**, *204*, 291.
(22) West, J. B.; Bradford, R. S.; Eversole, J. D.; Jones, C. R. *Rev. Sci. Instrum.* **1975**, *46*, 164.
(23) Gerstenkorn, S.; Luc, P. Atlas du Spectre d'Absorption de la Molécule d'Iode. Laboratoire Aimé-Cotton, CNRS II, France, 1978.
(24) Gerstenkorn, S.; Luc, P. *Rev. Phys. Appl.* **1979**, *14*, 791.
(25) Gerö, L. *Z. Phys.* **1935**, *93*, 669.
(26) Albritton, D. L.; Schmeltekopf, A. L.; Zare, R. N. *J. Mol. Spectrosc.* **1977**, *67*, 132.
(27) Coxon, J. A. *J. Mol. Spectrosc.* **1978**, *72*, 252.